DYNAMIC PASSIVE PRESSURE ON ABUTMENTS AND PILE CAPS

PI's Profs. Rollins and Gerber

Quarterly Report Jan. 2009-March 2009

Work this Quarter

During this quarter work has continued on the remaining two work tasks: Tasks 5 and Task 6. Final reports are presently being prepared for both tasks. A brief overview of the results of the work this quarter is provided below and more detailed reports are provided in the remainder of the report.

Task 5 Work (Tests at SLC Airport with Varying Backfill Types and Geometeries)

Work this quarter has focused on evaluating the passive resistance for the pile cap with different backfill conditions. The measured load-displacement response has been compared to curves predicted using three methods: the LSH method programmed in the computer program ABUTMENT, the log-spiral method with a hyperbolic load-displacement curve as programmed into the program PYCAP, and the CALTRANS standard design method. The subsequent report (Work Task 5, Section 1) highlights the results for the densely compacted clean sand backfill, the loosely compacted clean sand backfill, and the densely compacted fine gravel.

Other work has focused on evaluating the effect of pile cap height on passive earth resistance. This evaluation was done by comparing the test with the densely compacted clean sand backfill at the Airport site with the test conducted at South Temple by Cole and Rollins with a similar backfill. The subsequent report (Work Task 5, Section 2) presents preliminary results of this evaluation.

Task 6 Work (MSE Wingwall Tests)

Work for this quarter has focused on two areas: (1) Analysis of the pressure plate data on the face of the pile cap and (2) Analysis of the strain gauge data on the MSE steel reinforcing grids. The pressure plate results indicate that pressure distributions on the wall face are more complicated than the simple triangular distribution assumed in design. 3-D end effects increase the passive pressure near the edges of the pile cap. Therefore, the effective width of the pile cap must be used to obtain the total force rather than the actual width of the cap using the measured soil pressure near the center of the cap. The strain gauge data on the steel reinforcing grids indicate that the full pull-out resistance of the grid was developed during the load tests and the grids experienced pull-out failure even though the grids had a static safety factor of 1.5. The pull-out failure led to displacement of the MSE wall panels as development of passive pressure on the pile-backfill interface produced increases in the pressure on the MSE wingwalls. No design procedure is presently available which allows this pressure to be determined. Additional tests using reinforcement grids with higher factors of safety would be highly desirable.

Plans for the Next Quarter

We anticipate that draft final reports will be completed for the last two work tasks during the next quarter which will complete the work for this project. However, several issues have been identified during this study which could justify additional testing. Sponsors from several states have expressed interest in extending the work period by one to two years so that additional testing can be performed and some additional funding can be added to the pooled fund study. We anticipate that some funds will remain at the end of this study which could also be used to support this work. Additional tests would include (1) laboratory testing of the pile-pile cap connections which could evaluate full moment capacity. This could not be achieved in the field tests because of pile pull-out. (2) Field tests with MSE wingwalls having higher factors of safety to prevent pull-out. Reinforcement pull-out and MSE wall translation led to a stagnation of the passive force during the pile cap testing. No method currently exists to predict this behavior or the increase in pressure on MSE wingwalls produced by loading of the pile cap/abutment. Additional field tests could readily be performed with reinforcing grids having progressively higher factors of safety to evaluate performance and define improved design methods. (3) Field tests of skewed abutments. Skewed abutments develop normal and shear stresses on an abutment wall which are not well understood at present. The existing pile cap could easily be modified to allow these tests to be performed. Since a significant cost of these tests is associated with construction of the pile cap and reaction system, additional tests can now be performed with greater economy.

Budget Considerations

At the end of the quarter approximately $230,000 had been expended on work associated with Tasks 1-6. The total budget associated with all the project tasks is $265,395. Therefore, approximately 87% of the budget has been spent for these tasks. We estimate that approximately 90% of the work on the project has now been completed. Therefore, we anticipate that the project will be completed within the total budget.

WORK TASK 5 SUMMARY

EVALUATION OF PASSIVE EARTH RESISTANCES

1.1 GENERAL

Several methods are available to calculate the passive earth force (pressure) versus displacement relationship for the backfill soils. In this work, passive earth resistances were calculated using a modified version of the spreadsheet program PYCAP developed by Duncan and Mokwa (2001), the computer program entitled ABUTMENT which implements the LSH method presented by Shamshabadi et al. (2007), and the linear elastic demand method developed by CALTRANS. These calculated earth resistances are then compared to those measured during the pile cap lateral load tests.

1.2 CALCULATION METHODOLOGIES

1.2.1 PYCAP Methodology

Duncan and Mokwa (2001) presented a method in which the ultimate passive force (pressure) from a soil backfill is determined using the log-spiral method while the force versus displacement curve is based on a hyperbolic load-displacement relationship where initial loading stiffness (k_{max}) is based on the solution for a laterally loaded plate embedded in an elastic half-space (Douglas and Davis, 1964). The methodology has been implemented by Mokwa using an EXCEL spreadsheet entitled PYCAP.

Input parameters include soil properties such as soil friction angle (ϕ), cohesion (c), soil-foundation interface friction (δ), an adhesion factor (α), initial soil modulus (E_i), poisson's ratio (ν), and in-situ unit weight (γ). The inputs describing the foundation geometry are the foundation height (H), width (b), embedment depth (z), surcharge (q) and failure displacement divided by cap height (Δ_{max}/H).

The soil friction angle and cohesion, as well as the interface friction angle, were generally determined from direct shear testing. Initial soil modulus was found using the stress-strain unloading/reloading curve of a one-dimensional consolidation test and confirmed by comparing with typical values. Values for Possion’s ratio were selected from typical values. Specific

values for each parameter used in analyses will be presented subsequently. Three-dimensional loading effects are accounted for using the factor (R_{3D}) developed by Brinch-Hansen (1966). Along with a load-displacement curve of the passive earth pressure, PYCAP has several other outputs, including the soil loading stiffness (k_{max}), the hyperbolic failure ratio (R_f) which is derived from Δ_{max}/H, and the coefficient of passive earth pressure (K_p) from the log-spiral method of calculating passive soil resistance.

1.2.2 ABUTMENT (LSH) Methodology

In this methodology, the ultimate pressure of the backfill is determined by dividing the backfill soil into slices and then satisfying force-based, limit-equilibrium equations for mobilized logarithmic-spiral failure surfaces. Displacement is determined using a modified hyperbolic stress-strain relationship. This methodology, referred to as the LSH method and developed by Shamshabadi et al. (2007), has been incorporated by Shamshabadi into the computer program ABUTMENT.

Input parameters are soil properties and foundation geometry. The soil properties needed are internal friction angel (ϕ), soil cohesion (c), soil-foundation interface friction (δ), in-situ unit weight (γ), poisson's ratio (ν), and strain at 50% strength (ε_{50}). An additional failure ratio (R_f) parameter must be defined which helps control the sharpness of the hyperbolic curve. Different from the R_f values used in some hyperbolic soil models, this value typically ranges from 0.95 to 0.98. Output from the program includes the load-displacement curve and the passive horizontal earth pressure coefficient. Most of the soil input parameters were selected in the same way that they were chosen for the analyses using PYCAP. The strain parameter is difficult to precisely define but was estimated using the stress-strain loading curve of a one-dimensional consolidation test and then compared with values shown for similar backfill materials in Shamshabadi et al. (2007). Within the computer program, the log-spiral force method of calculation was used with the "composite" option while the stresses and strains were calculated using the "modified hyperbolic" option. Three-dimensional end effects were accounted for using an effective foundation width determined using the same Brinch-Hansen (1966) relationships as used in the PYCAP based analyses.

1.2.3 CALTRANS Method

Based on full scale tests conducted at UC Davis (Maroney 1995), CALTRANS developed a method to determine the initial stiffness and ultimate passive resistance for abutment backfill to use in standard design work. The initial stiffness (K_{abut}) and ultimate force (P_{ult}) are determined using

$$K_{abut} = 11.5 \frac{kN/mm}{m} * w_{abut} * \left(\frac{h}{1.7}\right)$$

Equation 1 and

$$P_{ult} = 239\ kPa * A_{abut} * \left(\frac{h}{1.7}\right)$$

Equation 2

$$K_{abut} = 11.5\frac{kN/mm}{m} * w_{abut} * \left(\frac{h}{1.7}\right) \qquad K_{abut} = 11.5\frac{kN/mm}{m} * w_{abut} * \left(\frac{h}{1.7}\right)$$

Equation 1

$$P_{ult} = 239\ kPa * A_{abut} * \left(\frac{h}{1.7}\right) \qquad P_{ult} = 239\ kPa * A_{abut} * \left(\frac{h}{1.7}\right)$$

Equation 2

where w_{abut} is the width of the abutment, h is the height of the abutment and A_{abut} is the area of the abutment (with a dimension expressed in terms of meters). The load-displacement relationship follows the initial stiffness and then becomes constant when the ultimate pressure is exceeded. The method scales different abutment heights linearly to the height of the test abutment and does not account of changes in backfill material. In fact, there are no soil properties used in the method. For the geometry of the test pile cap, this method indicates the initial slope is to be 39 kN/mm and the ultimate passive resistance is to be approximately 1360 kN.

1.3 OAD-DISPLACEMENT CURVES FOR DENSELY COMPACTED CLEAN SAND BACKFILL

1.3.1 Measured Response

Figure 0-1 shows three load-displacement responses (curves) for the pile cap: one for the response with the backfill in place (referred to as the total response), one for the response with no backfill present (referred to as the baseline response), and one showing the passive earth response of the backfill (obtained by subtracting the baseline response from the total response). The curves show that total response and baseline response increase at different rates until approximately 48 to 50 mm of displacement (depending upon visual interpretation). By this point, the backfill response levels off as the baseline and total response increase at approximately the same rate. This leveling off is interpreted as the point when the backfill material is at failure. Hence, the ultimate

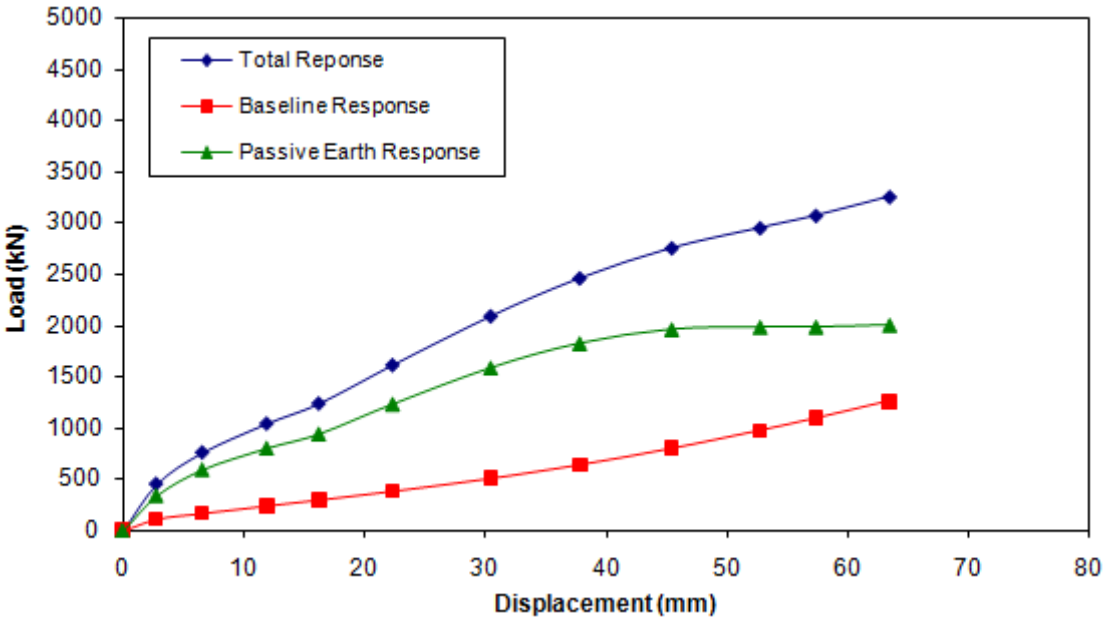

Figure 0-1 Total, baseline, and passive earth responses for pile cap with densely compacted clean sand backfill

passive resistance of the backfill is developed at a displacement of approximately 50 mm, which corresponds to a displacement to wall height ratio (Δ_{max}/H) of about 0.03.

1.3.2 Calculated Response Using PYCAP

Passive earth resistance was calculated using the modified PYCAP spreadsheet. Table 0-1 summarizes key inputs and outputs for several cases analyzed while Figure 0-2 shows the measured and calculated passive resistance curves for each case. Case I is based strictly on laboratory-determined ultimate values for shear strength, interface friction angle (which was similar for both peak and ultimate strength states) and initial modulus. Case II is identical to Case I except that the internal friction angle is based on peak strength. Case III is similar to Case I, except an interface friction angle has been changed to match the δ/ϕ ratio determined by Cole and Rollins (2006) for a different pile cap using the same type of backfill material, and the initial modulus has also been changed to better fit the initial slope of the measured data. For Case I, the calculated ultimate passive resistance is slightly less than the measured ultimate passive resistance. Case II predicts an ultimate passive resistance 35% greater than Case I. Case III matches the initial slope and the ultimate value of the measured resistance line. Overall the hyperbolic model used in PYCAP appears to match well with the measured data when ultimate shear strength parameters and a δ/ϕ ratio of 0.75 are used.

Table 0-1 Summary of PYCAP parameters for densely compacted clean sand backfill

Parameter	Case I	Case II	Case III

ϕ (°)	40.5	43.3	40.5
c (kPa)	0	0	0
δ (°)	29	29	30.4
γ_m (kN/m^3)	18.3	18.3	18.3
E (kPa)	39700	39700	28700
ν	0.3	0.3	0.3
k (kN/mm)	240	240	170
Δ_{max} (mm)	50	50	50
Δ_{max}/H	0.030	0.030	0.030
R_f	0.84	0.79	0.77
R_{3D}	1.83	1.97	1.85
K_p	13.8	17.3	14.4

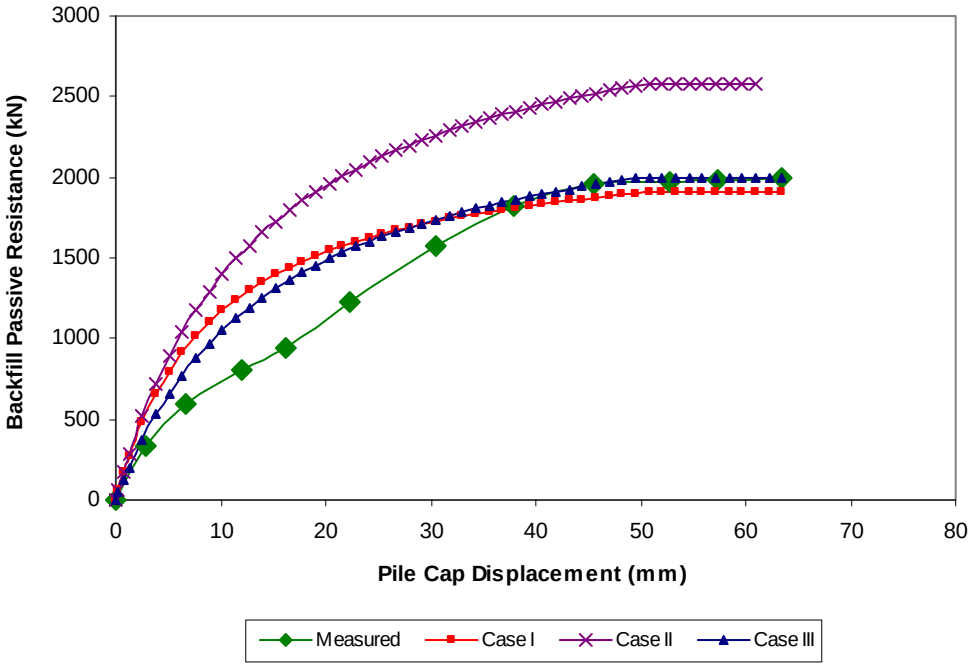

Figure 0-2 Comparison of measured and PYCAP-based calculated passive resistance for densely compacted clean sand backfill

1.3.3 Calculated Response Using ABUTMENT (LSH)

Passive earth resistance was also calculated using ABUTMENT and the LSH methodology. Table 0-2 summarizes key inputs and outputs for several cases analyzed while Figure 0-3 shows

the measured and calculated passive resistance curves for each case. Case I is based strictly on laboratory-determined values for ultimate shear strength and is the same as Case I in analyses performed using PYCAP. Case II is the same as Case I except the peak friction angle has been used. The measured data lies between these two curves. Case III is a result of adjusting Case I to include some cohesion and match the peak resistance. A relatively small amount, 4.0 kPa, was used. This value is the same value as was used by Shamshabadi et al. (2007) in their analyses of Rollins and Cole (2006) pile cap test results with a similar backfill material. Case IV is the result of doubling the strain parameter to obtain a better match with the initial portion of the curve, but good agreement was not obtained and further increase would result in excessive displacement when the ultimate resistance is reached. The best match was obtained in Case III using the ultimate friction angle and a small amount of cohesion.

Table 0-2 Summary of LSH parameters for densely compacted clean sand backfill

Parameter	Case I	Case II	Case III	Case IV
ϕ (°)	40.5	43.3	40.5	40.5
c (kPa)	0	0	4.0	4.0
δ (°)	29	29	29	29
γ_m (kN/m^3)	18.3	18.3	18.3	18.3
ε_{50}	0.002	0.002	0.002	0.004
ν	0.3	0.3	0.3	0.3
R_f	0.98	0.98	0.98	0.98
R_{3D}	1.83	1.97	1.83	1.83
K_{ph}	10.8	13.4	13.2	13.2

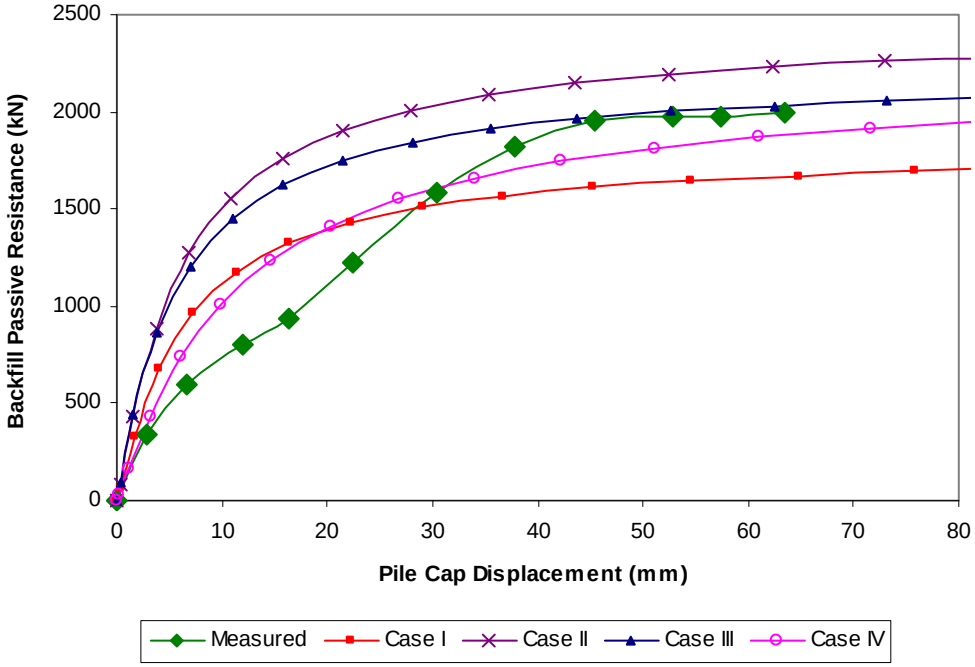

Figure 0-3 Comparison of measured and LSH-based calculated passive resistance for densely compacted clean sand backfill

1.3.4 Calculated Response Using CALTRANS Method

Passive earth resistance based on the CALTRANS method is shown in Figure 0-4. The method under-predicts peak passive resistance by approximately 30%. The initial slopes of the calculated and measured pressure are generally comparable, although the calculated pressure in that region is lower than the measured pressure.

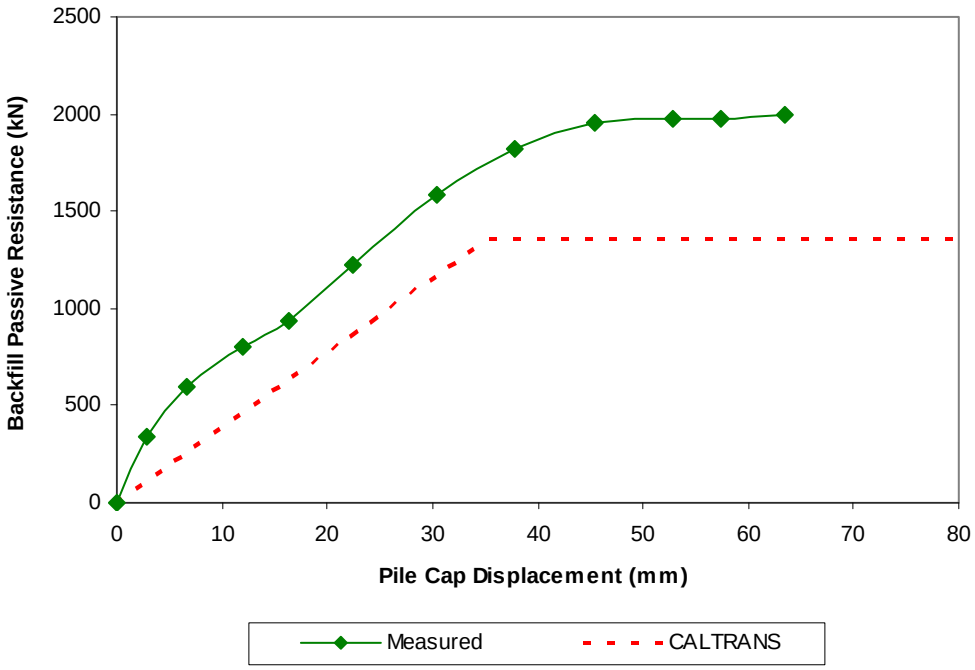

Figure 0-4 Comparison of measured and CALTRANS-based passive resistance for densely compacted clean sand backfill

1.4 LOAD-DISPLACEMENT CURVES FOR LOOSELY COMPACTED CLEAN SAND BACKFILL

1.4.1 Measured Response

Figure 0-5 shows three load-displacement response curves for the pile cap: one for the response with backfill in place (referred to as the total response), one for the response with no backfill present (referred to as the baseline response), and one showing the passive earth response of the backfill (obtained by subtracting the baseline response from the total response. This figure shows that after the initial push, the loosely compacted sand backfill provides an additional resistance which is slightly less than the resistance initially provided by the piles and cap acting by themselves. A peak passive force appears to possibly develop by about 38 mm of displacement which is actually less than the displacement at which the densely compacted sand developed full passive pressure. This is unexpected, given that Clough and Duncan (1991) stated that a loose or medium dense material will require two to four times more displacement to mobilize that a dense material. Although the passive pressure appears to peak at 38 mm, it is unknown for certain if the passive pressure might have slowly continued to increase had the test continued to a higher displacement levels. Unfortunately, there was an equipment malfunction which ended the test prematurely and prevented data collection for greater displacement levels. In the figure it can be seen that a significant amount of this pressure seems to have developed by 6 mm of displacement, after which the earth pressure appears to drop and then later recovers. This behavior is surprising and may be due to the effects of cyclic and dynamic loadings, or

possibly even a small error in the baseline response which effect is magnified since the passive resistance of the backfill is also relatively small.

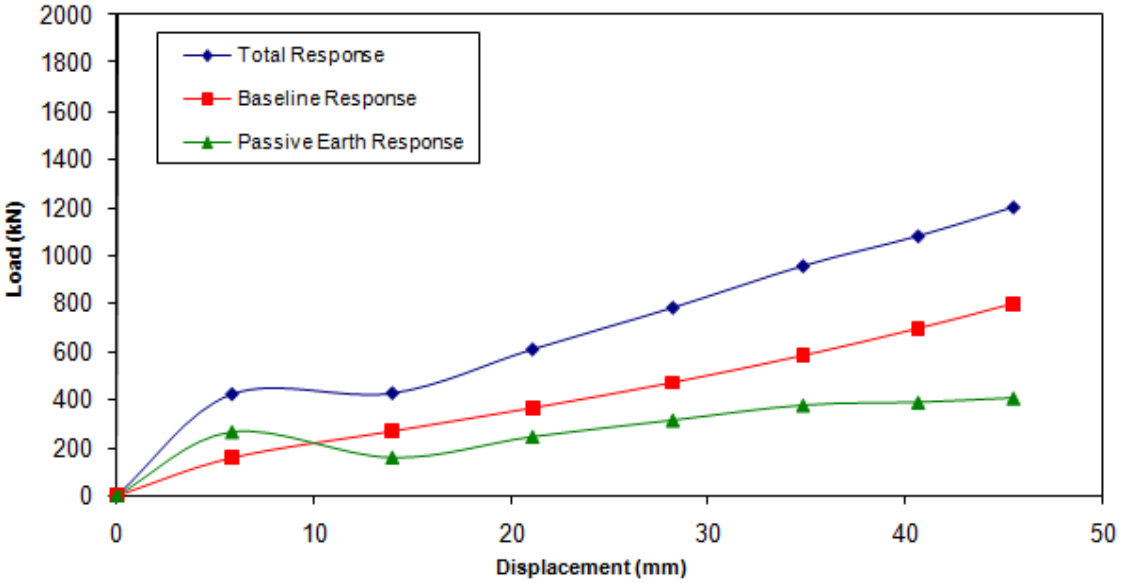

Figure 0-5 Total, baseline and passive earth responses for the pile cap with loosely compacted clean sand backfill

1.4.2 Calculated Response Using PYCAP

Passive earth resistance was calculated using the modified PYCAP spreadsheet. Table 0-3 summarizes key inputs and outputs for the various cases analyzed while Figure 0-6 shows the measured and the calculated passive resistance curves for each case. Case I is the best estimate case based on laboratory testing. The ultimate passive resistance from Case I is 189% greater than the measured resistance. The initial modulus value used in Case I is consistent with the preloaded or compacted range given by Duncan and Mokwa (2001). Case II is similar to Case I, except that the initial soil modulus was lowered to match the initial measure slope and the soil friction angle was lowered to 25.5 degrees with a similar δ/ϕ ratio to better match the ultimate passive resistance. The lowered modulus value is within the normal range suggested by Duncan and Mokwa (2001). The friction angle needed to match the measured pressure is quite a bit lower than what would likely be expected. According to the NAVFAC manual (US Navy, 2006), which likely has some degree of conservatism, a SW material with a relative density of 57% would have a friction angle of approximately 34 degrees. This suggests that the parameters used to obtain the match in Case II are not likely to be realistic. Case III is similar to Case I, except the ultimate strength friction angle has been used along with an interface friction angle of zero (corresponding to Rankie's earth pressure conditions). The similarity between the load-displacement curve for Case III and the measured curve strongly suggests that for this particular loosely compacted backfill and loading conditions, the amount of mobilized interface friction is negligible.

Table 0-3 Summary of PYCAP parameters for loosely compacted clean sand backfill

Parameter	Case I	Case II	Case III
ϕ (°)	37.3	25.5	37.3
c (kPa)	0	0	0
δ (°)	27	18	0
γ_m (kN/m^3)	16.5	16.5	16.5
E (kPa)	30600	15800	30600
ν	0.3	0.3	0.3
k (kN/mm)	190	120	190
Δ_{max} (mm)	38	38	38
Δ_{max}/H	0.023	0.023	0.023
R_f	0.84	0.91	0.90
R_{3D}	1.67	1.34	1.36
K_p	10.1	3.9	4.1

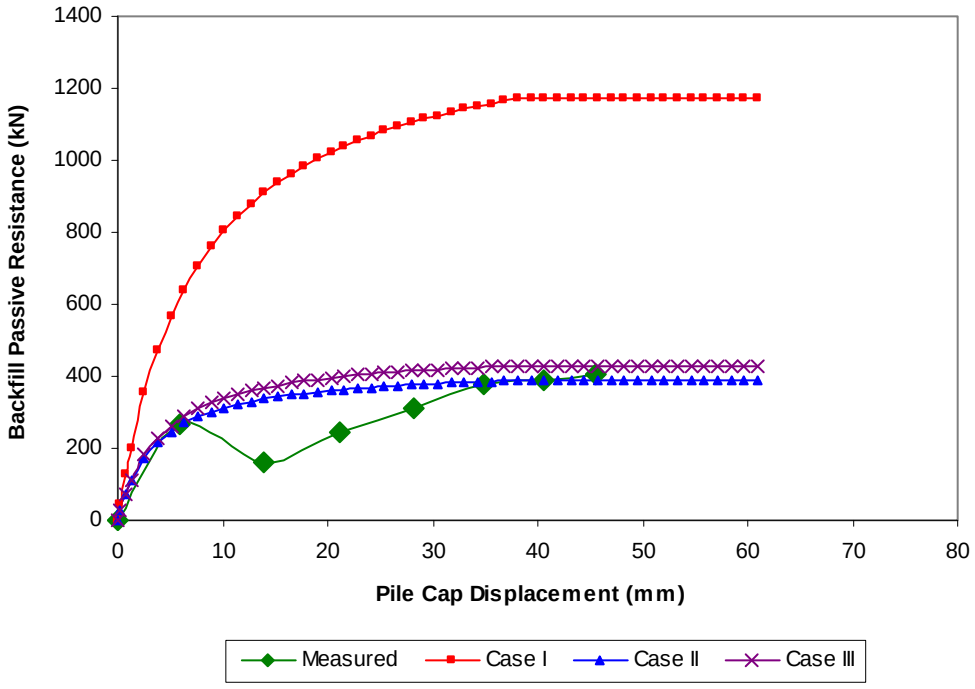

Figure 0-6 Comparison of measured and PYCAP-based calculated passive resistance for loosely compacted clean sand backfill

1.4.3 Calculated Response Using ABUTMENT (LSH)

Passive earth resistance was also calculated using the LSH method. Table 0-4 summarizes key inputs and outputs for several cases analyzed while Figure 0-7 shows the measured and calculated passive resistance curves for each case. Case I is based on the laboratory direct shear test results for ultimate strength, and produces a poor match with the measured earth pressure curve. In Case II, the friction angle has been iteratively reduced with a similar δ/ϕ ratio to provide a better fit with the data, and this reduced friction angle is same to the reduced friction angle used in the PYCAP-based analyses. A better match would be obtained by increasing the angle a degree or two or adding a small amount of cohesion. In Case III, the ultimate strength parameters have been used, but the interface friction angle has been set to zero. With these conditions, the Case III

Table 0-4 Summary of LSH parameters for loosely compacted clean sand backfill

Parameter	Case I	Case II	Case III	Case IV
ϕ (°)	37.3	25.5	37.3	37.3
c (kPa)	0	0	0.0	0.0
δ (°)	27	18	0	0
γ_m (kN/m^3)	16.5	16.5	16.5	16.5
ε_{50}	0.004	0.004	0.004	0.002
ν	0.3	0.36	0.36	0.36
R_f	0.98	0.98	0.98	0.98
R_{3D}	1.67	1.34	1.36	1.36
K_{ph}	8.4	3.7	4.1	4.1

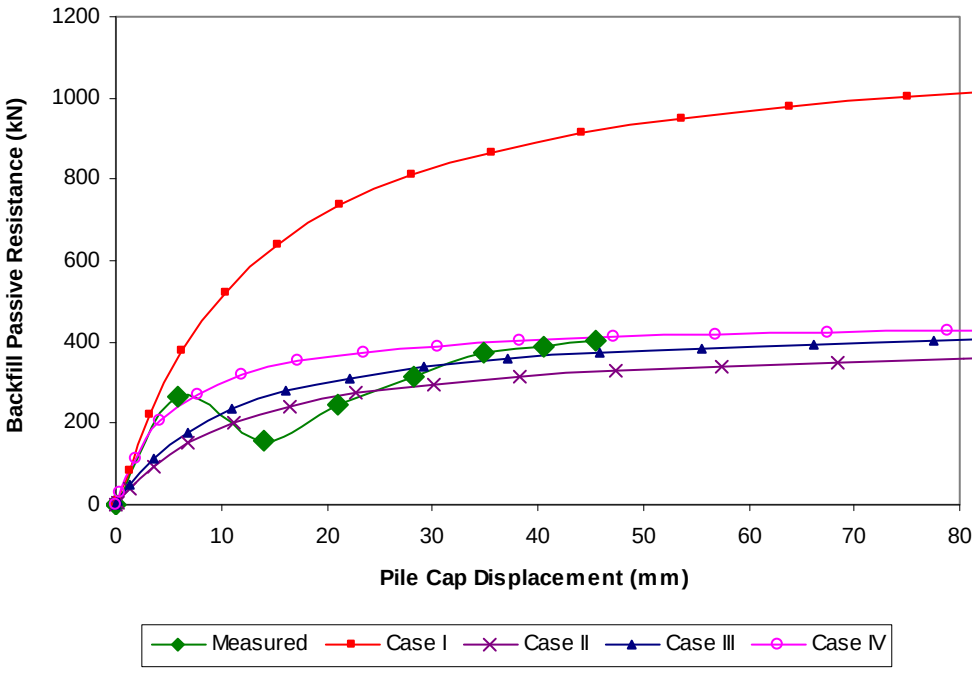

Figure 0-7 Comparison of measured and LSH-based calculated resistance for loosely compacted clean sand backfill

theoretical curve under-predicts the maximum passive resistance by about 7% but also fails to realistically model the initial portion of the loading curve. The under-prediction of the maximum passive resistance appears to be in part due to the strain value ε_{50} (which is assumed in the LSH method to be approximately 1/31 of the failure strain). In Case IV, the strain value from Case III has been reduced in half, producing a much better overall match. Again, it appears that the theoretical prediction of passive resistance overestimates the actual value unless either a lower friction angle is used or the interface friction is significantly reduced or eliminated.

1.4.4 Calculated Response Using CALTRANS Method

Passive earth resistance based on the CALTRANS method is shown in Figure 0-8. In this case, the method over-predicts peak passive resistance by 250%.

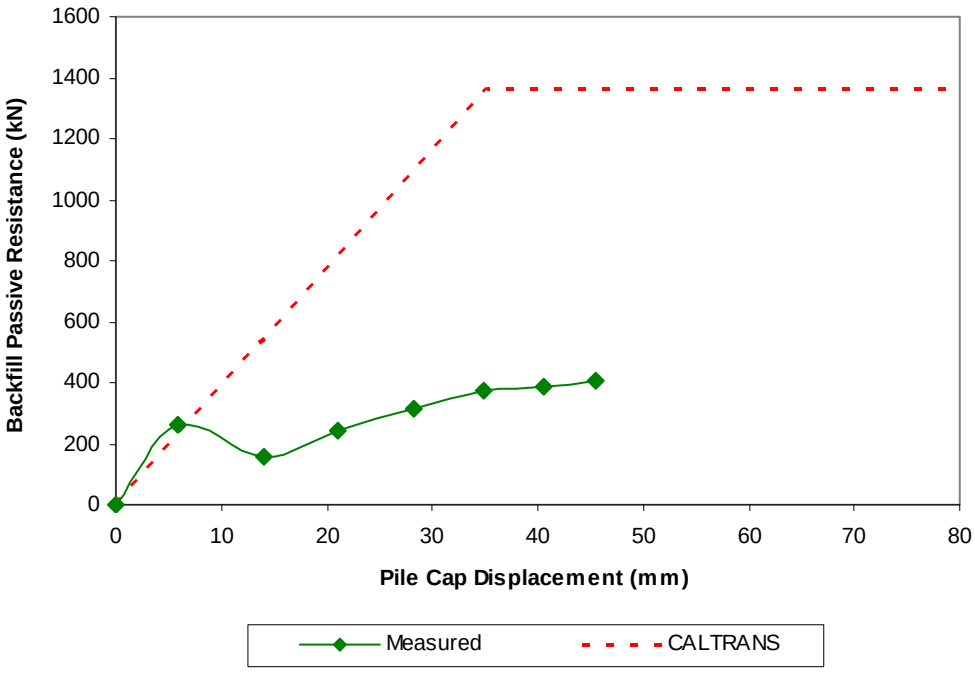

Figure 0-8 Comparison of measured and CALTRANS-based passive resistance for loosely compacted clean sand backfill

1.5 LOAD-DISPLACEMENT CURVES FOR DENSELY COMPACTED FINE GRAVEL BACKFILL

1.5.1 Measured Response

Figure 0-9 shows three load-displacement responses (curves) for the pile cap: one for the response with the backfill in place (referred to as the total response), one for the response with no backfill present (referred to as the baseline response), and one showing the passive earth response of the backfill (obtained by subtracting the baseline response from the total response). The curves show that total response and baseline response increase at different rates until approximately 62 mm of displacement. By this point, the backfill response levels off as the baseline and total response increase at approximately the same rate. This leveling off is interpreted as the point when the backfill material is at failure. Hence, the ultimate passive resistance of the backfill is developed at a displacement of approximately 62 mm, which corresponds to a displacement to wall height ratio (Δ_{max}/H) of about 0.037.

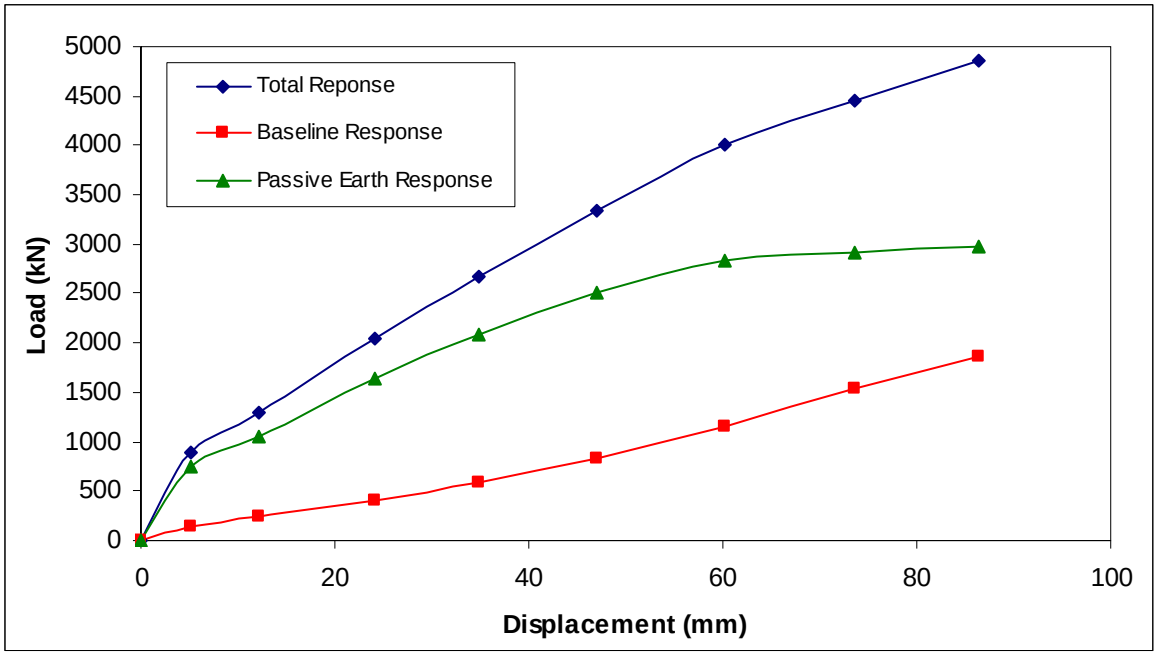

Figure 0-9 Total, baseline, and passive earth responses for pile cap with densely compacted fine gravel backfill

1.5.2 Calculated Response Using PYCAP

Passive earth resistance was calculated using the modified PYCAP spreadsheet. Table 0-5 summarizes key inputs and outputs for several cases analyzed while Figure 0-10 shows the measured and calculated passive resistance curves for each case. Case I is based strictly on laboratory-determined ultimate values for shear strength, interface friction angle (which was

similar for both peak and ultimate strength states, with a laboratory based δ/ϕ ratio of about 0.61) and initial modulus. For Case I, the calculated load-displacement curve greatly exceeds the measured curve. Parameters for Case II are identical to Case I except that the cohesion has been neglected. The resulting load-displacement curve is closer to, but still greatly more than, the measured curve. Case III is similar to Case I, except the interface friction angle has been iteratively changed to obtain a good match between the calculated and measured load-displacement curves. Case IV uses a friction angle based on an in-situ direct shear test staged using one sample over three normal pressures. The apparent cohesion of 19.6 kPa from that test has been neglected and the δ/ϕ ratio is the same as used previously. The resulting curve for Case IV provides a reasonable match with the measured curve.

Table 0-5 Summary of PYCAP parameters for densely compacted fine gravel backfill

Parameter	Case I	Case II	Case III	Case IV
ϕ (°)	50.0	50.0	50.0	44.0
c (kPa)	13.2	0	13.2	4.0
δ (°)	31	31	8	27
γ_m (kN/m^3)	21.7	21.7	21.7	21.7
E (kPa)	32100	32100	32100	32100
N	0.3	0.3	0.3	0.3
k (kN/mm)	190	190	190	190
Δ_{max} (mm)	62	62	62	62
Δ_{max}/H	0.037	0.037	0.037	0.037
R_f	0.30	0.48	0.76	0.75
R_{3D}	2.00	2.00	1.72	1.95
K_p	35.7	35.6	11.2	17.0

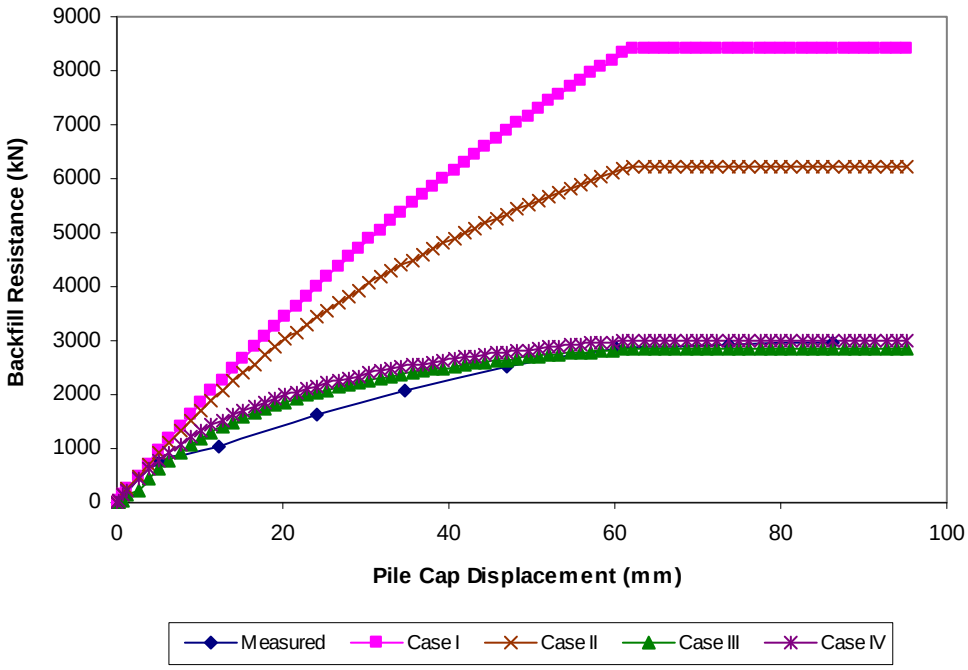

Figure 0-10 Comparison of measured and PYCAP-based calculated passive resistance for densely compacted fine gravel backfill

1.5.3 Calculated Response Using ABUTMENT (LSH)

Passive earth resistance was also calculated using ABUTMENT and the LSH methodology. Table 0-6 summarizes key inputs and outputs for several cases analyzed while Figure 0-11 shows the measured and calculated passive resistance curves for each case. Case I is based strictly on laboratory-determined ultimate values for shear strength, interface friction angle (which was similar for both peak and ultimate strength states, with a δ/ϕ ratio of about 0.61) and initial modulus. These are the same parameters used in Case I with the PYCAP analysis. For Case I, the calculated load-displacement curve greatly exceeds the measured curve. Cases II and III represent the same parameters used in the corresponding cases with the PYCAP analysis. If cohesion is included, the interface friction angle must be greatly reduced to obtain a good match. Case IV uses a friction angle based on an in-situ direct shear test staged using one sample over three normal pressures. In this case, the majority of the apparent cohesion from that test has been neglected and an amount of 4.0 kPa has been used. This value is the same as was used by Shamshabadi et al. (2007) in their analyses of Cole and Rollins (2006) pile cap test results with a similar backfill material. The resulting curve for Case IV provides a good match with the measured curve. While Case III provides the best match with the measured curve (since the interface friction angle was iteratively determined to obtain such a match), the parameters represented by Case IV provide the most reasonable description of the measured load-displacement curve. In all cases, the poorest match occurs in the mid portion of the load-displacement curves. The PYCAP and ABUTMENT programs appear to produce similar results if a small amount of cohesion is used in ABUTMENT when none is used in PYCAP.

Table 0-6 Summary of LSH parameters for densely compacted fine gravel backfill

Parameter	Case I	Case II	Case III	Case IV
ϕ (°)	50.0	50.0	50.0	44.0
c (kPa)	13.2	0	13.2	4.0
δ (°)	31	31	8	27
γ_m (kN/m^3)	21.7	21.7	21.7	21.7
ε_{50}	0.004	0.004	0.004	0.004
N	0.3	0.3	0.3	0.3
R_f	0.98	0.98	0.98	0.98
R_{3D}	2.00	2.00	1.72	1.95
K_{ph}	36.3	25.0	17.7	16.0

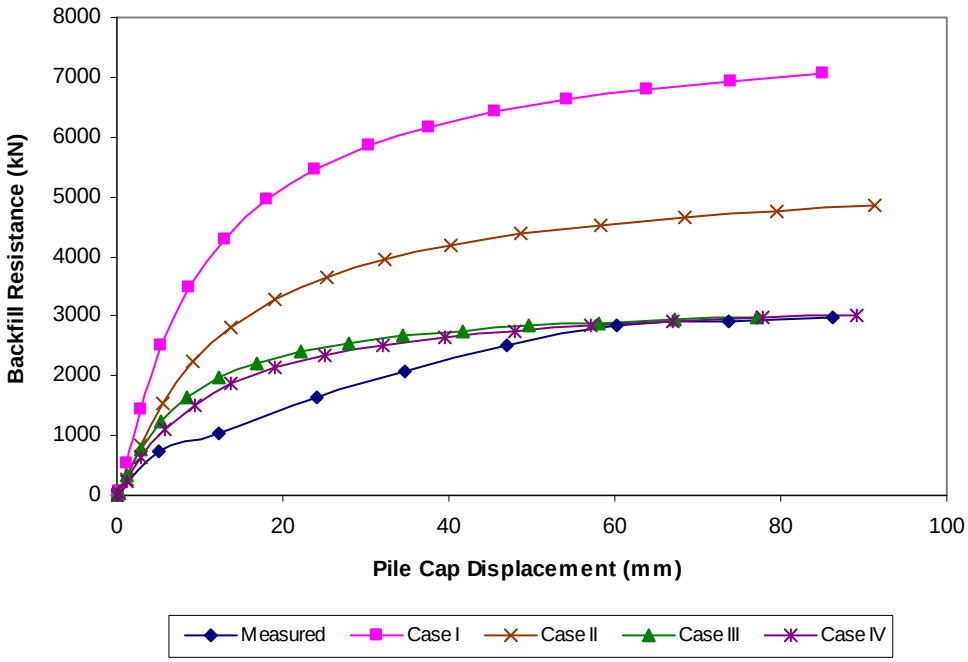

Figure 0-11 Comparison of measured and LSH-based calculated passive resistance for densely compacted fine gravel backfill

1.5.4 Calculated Response Using CALTRANS Method

Passive earth resistance based on the CALTRANS method is shown in Figure 0-12. In this case, the method under-predicts peak passive resistance by approximately 50%.

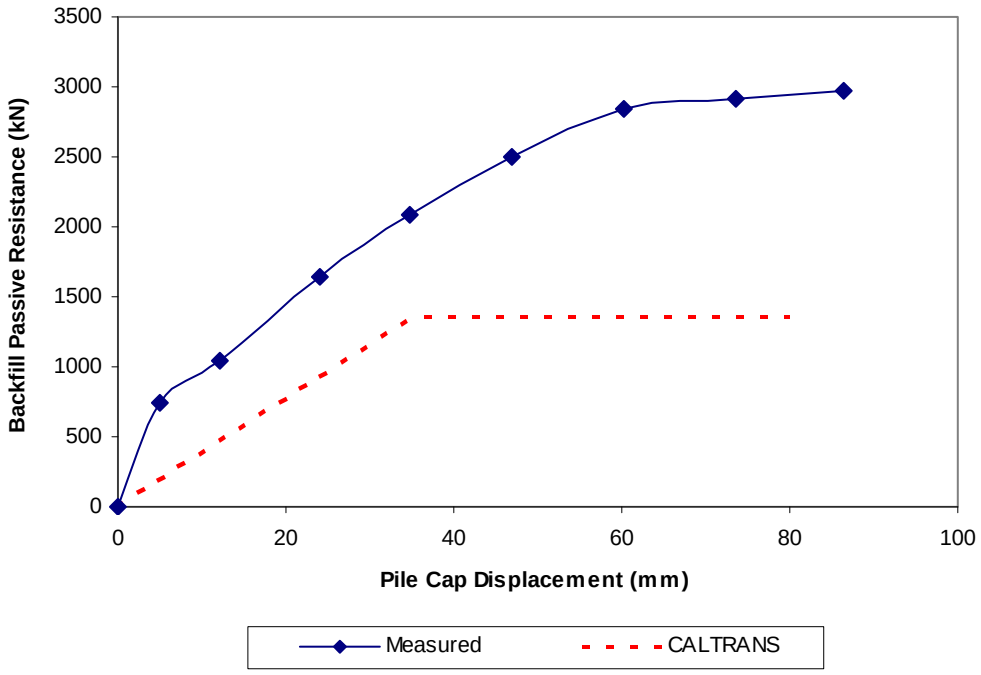

Figure 0-12 Comparison of measured and CALTRANS-based passive resistance for densely compacted fine gravel backfill

2. 0 EFFECT OF PILE CAP HEIGHT

Cole and Rollins (2006) conducted a lateral load test on a 1.12 m high pile cap with a densely compacted clean sand backfill similar to that used in the current tests with a 1.68 m high pile cap at the Salt Lake City International Airport. By comparing the results of these two tests, the effect of pile cap height on passive earth pressure can be evaluated. Parameters from the test of Cole and Rollins at the South Temple / I-15 site are shown in Table 2-7 together with the corresponding parameters from the test at the Airport. Soil parameters are based on laboratory values and have not been adjusted to improve the match between measured and theoretical passive earth pressures.

Table 2-7 Summary of load test parameters from South Temple and Airport sites

Parameter	South Temple	Airport
Cap height, H (m)	1.12	1.68
Cap width, B (m)	5.18	3.35
Horiz. passive earth force,P_{ph} (kN)	1090	1966
Friction angle, ϕ (°)	39	40.5
Cohesion, c (kPa)	0	0
Interface friction angle, δ (°)	30	29
Moist unit weight, γ_m (kN/m^3)	18.4	18.3
Disp. for max. soil force, Δ_{max} (mm)	38	50
Δ_{max}/H	0.034	0.030
Three dimensional factor, R_{3D}	1.36	1.83
Passive earth pressure coeff., K_p	15.6	14.2
P-S passive earth force,P_{phps} (kN/m)	155	320

The horizontal passive earth force and displacement at which this force is developed are based on the load-displacement curves for the two tests shown in Figure 2-13 and Figure 2-14. The three-dimensional loading effect due to different pile cap face aspect ratios was determined using the correction factor (R_{3D}) developed by Brinch-Hansen (1966). The passive earth pressure coefficient was calculated using the expression shown in Equation 2-3, whereas the normalized or plane-strain passive earth force (i.e., passive earth force normalized per unit width after removing three dimensional effects) was calculated using Equation 2-4.

$$P_{ph} = \frac{1}{2}\left(K_p \gamma_m H\right) H \; B \; R_{3D} \cos(\delta) \qquad \textbf{Equation 2-3}$$

$$P_{phps} = \frac{P_{ph}}{B \; R_{3D}} \qquad \textbf{Equation 2-4}$$

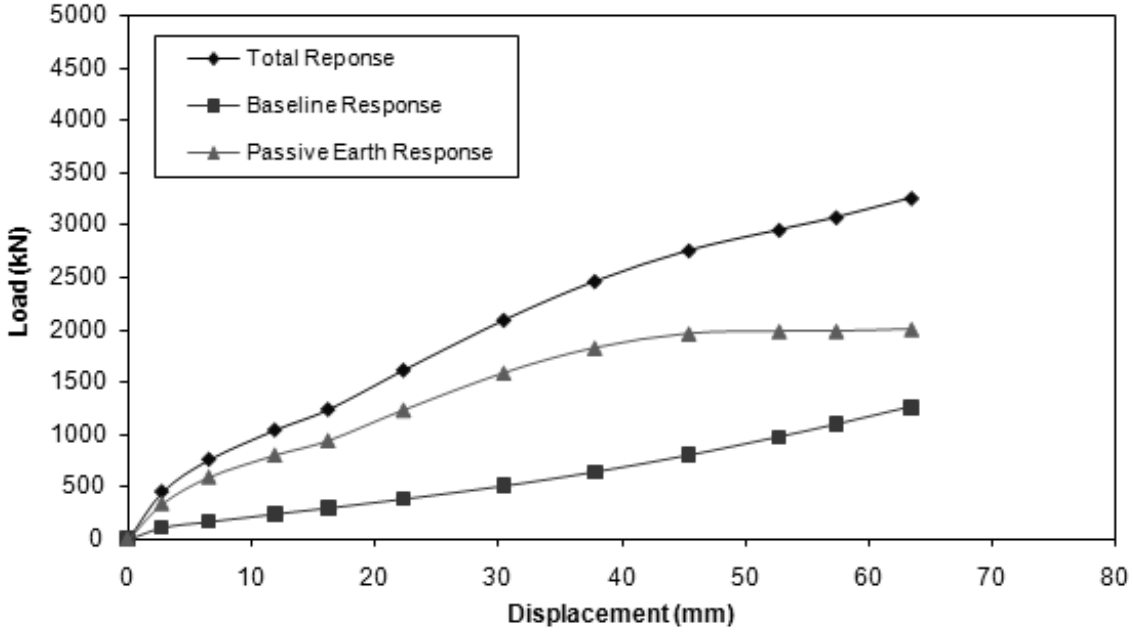

Figure 2-13 Load-displacement response for pile cap with densely compacted clean sand backfill at Airport site

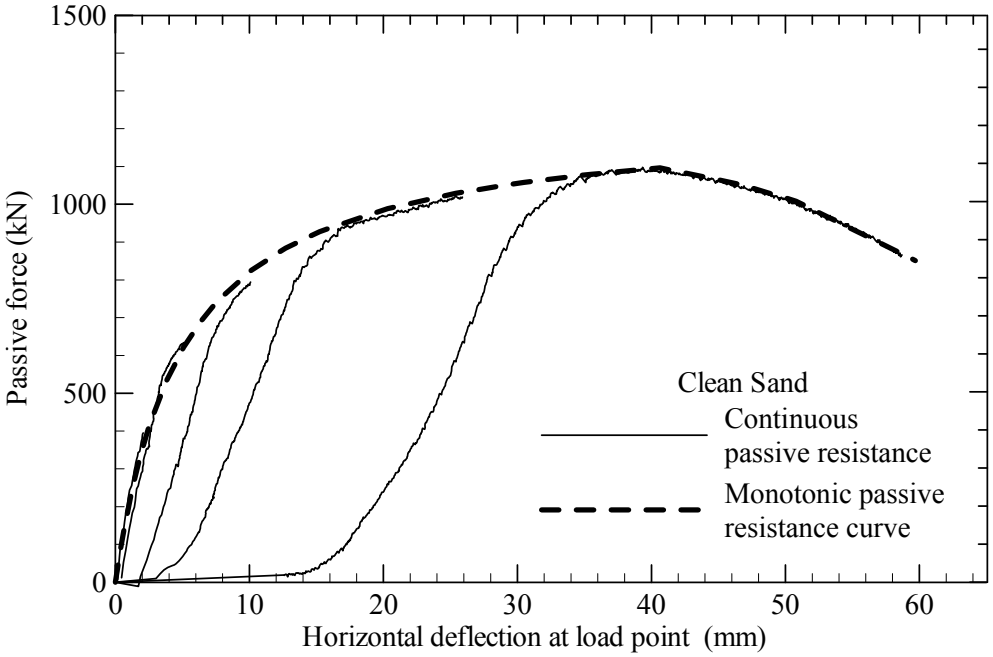

Figure 2-14 Load-displacement response for pile cap with densely compacted clean sand backfill at South Temple site (after Cole and Rollins, 2006)

From the data shown in Table 2-7, it can be seen that the passive earth pressure coefficients are quite similar (within 9%), despite some variances in the measured soil properties

at the two sites. This suggests that it is reasonable to compare the results of these two tests to assess the effect of pile cap height on the passive resistance of backfill soil.

Despite differing aspect ratios (B/H) of 4.6 and 2.0 for the South Temple and Airport pile caps, respectively, the displacement to height ratio (Δ_{max}/H) is similar for both caps, being on the order of 3%. Expressed in terms of an equivalent fluid pressure, the term $K_p \gamma_m$ is similar for both caps, being 287 and 260 kN/m^3, which averages to 274 kN/m^3. Hence, for pile caps of different heights with the same backfill material, the ratio Δ_{max}/H appears to be constant (as expected), and the passive earth force is closely a function of the square of the height (as indicated by earth pressure theory).

The two tests can also be compared to assess the effect of height on foundation stiffness. Unfortunately, the initial portion of the load-displacement curve for the Airport pile cap appears to be unusually soft (perhaps due to cyclic/dynamic loading effects), thus preventing a definitive comparison of initial stiffness conditions. However, a comparison of stiffness at the maximum passive earth resistance can be made. Using the relationship shown in Equation 2-5, the equivalent stiffness (k_{equiv}) for the South Temple and Airport backfills is approximately 4.08 and 10.67 kN/mm, respectively.

$$k_{equiv} = \frac{P_{phps}}{\Delta_{max}} \qquad \textbf{Equation 2-5}$$

Using the Airport pile cap whose height is 1.68 m (5.5 ft) as a reference, Equation 2-6 was used to determine an appropriate cap (wall) height scaling parameter, n.

$$k_{southtemple} = k_{airport}\left(\frac{H_{southtemple}}{H_{airport}}\right)^n \qquad \textbf{Equation 2-6}$$

An exponent, n, of 2.38 (about 19/8) satisfies Equation 4. Given the initial variation in earth pressure coefficients between the two sites and given that the height term is squared in Equation 1, and although wall height does somewhat effect the passive earth pressure coefficient determined by the log-spiral method, it seems reasonable to approximate the exponent n as 2.0, indicating that wall stiffness is a function of the square of the height ratio.

WORK TASK 6 SUMMARY

PRESSURE CELL INSTRUMENTATION AND TEST RESULTS

Pressure Cell Layout

Six 9 inch diameter pressure cells were used to measure the pressure distribution with depth from the backfill on the face of the pile cap. These pressure cells were placed with their centers at depths of 7.75. 18.5, 29.5, 41.0, 51.5, and 62.5 inches below the top of the pile cap in the center portion of the pile cap as shown in Fig 1. These stainless steel pressure cells were designed with a reinforced backplate to reduce point loading effects when directly mounting the cell to a concrete or steel structure. The cells utilize a electrical resistance type semi-conductor pressure transducer rather than a vibrating wire transducer to more accurately measure rapidly changing pressures. The cells were cast integrally with the pile cap, with their top surfaces being flush with the concrete face.

Pressure Plate Results for Load Test With MSE Wingwalls

The measured pressure distribution with depth for the test with MSE wingwalls is plotted in Figure 2 (a) for six pile cap displacement increments. As the displacement increases, the pressure increases; however, relatively little change is observed for displacements higher than about 1.98 inches when the maximum load is developed. The pressure distribution tends to have a bilinear shape with a lower slope at the top than at the bottom. This could result from lower confinement at the top of the wall due to pull-out of the MSE reinforcement or outward rotation of the MSE wall as discussed subsequently.

The force on the pile cap was computed by multiplying the pressure at each measurement elevation by the tributary area. The tributary area is the width of the pile cap times the vertical distance between pressure plates. The total force on the pile cap computed from the pressure plates is compared with the force measured by the actuators in the force-displacement curves plotted in Figure 2 (b). The two curves generally have similar shapes, although the force from the actuators is about 15 to 20% higher than that from the pressure plates. This discrepancy can likely be attributed to the assumption of uniform pressure across the width of the pile cap. Soil-structure analyses typically show stress concentrations near the ends of a concrete mat or pile cap. Since the pressure plates are near the center of the cap, they would not register this increased pressure near the ends and would, therefore, underestimate the total force on a horizontal segment of the pile cap.

Pressure Plate Results for Load Test Without MSE Wingwalls

The measured pressure distribution with depth for the test without MSE wingwalls is plotted in Figure 3 (a) for 11 pile cap displacement increments. As the displacement increases, the pressure increases; however, smaller increases are observed at higher displacements as the maximum load is approached. The pressure distribution tends to have a parabolic shape and there is a reduction in pressure at the base of the cap which suggests pile cap rotation.

The force on the pile cap was computed by multiplying the pressure at each measurement elevation by the tributary area as described previously. The total force on the pile cap computed from the pressure plates is compared with the force measured by the actuators in the force-displacement curves plotted in Figure 3 (b). The two curves generally have similar shapes; however, the force from the actuators is about 30% to 50% higher than that from the pressure plates. This is significantly more error than that observed for the pile cap with the MSE wingwalls. Once again, this discrepancy can likely be attributed to the assumption of uniform pressure across the width of the pile cap. Because the shear zones extend beyond the ends of the pile cap without wingwalls, greater stress concentrations would be expected to develop at the ends of the pile cap as illustrated in Figure 4. Since the pressure plates are near the center of the cap, they would not register this increased pressure near the ends and would, therefore, underestimate the total force on a horizontal segment of the pile cap. One method to account for the increased passive resistance due to 3-D end effects is to increase the effective width of the pile cap. The Brinch-Hansen equation and field observations suggest that the effective width of the pile cap for this geometry was between 18 to 19 ft, rather than the actual 11 ft cap width. When an effective cap width of 18 ft is used, the agreement between the total passive force computed from the pressure plates is reasonably close to that measured by the actuators.

Figure 1. Photograph of front face of pile cap before backfill placement showing layout of six pressure plates.

(a)

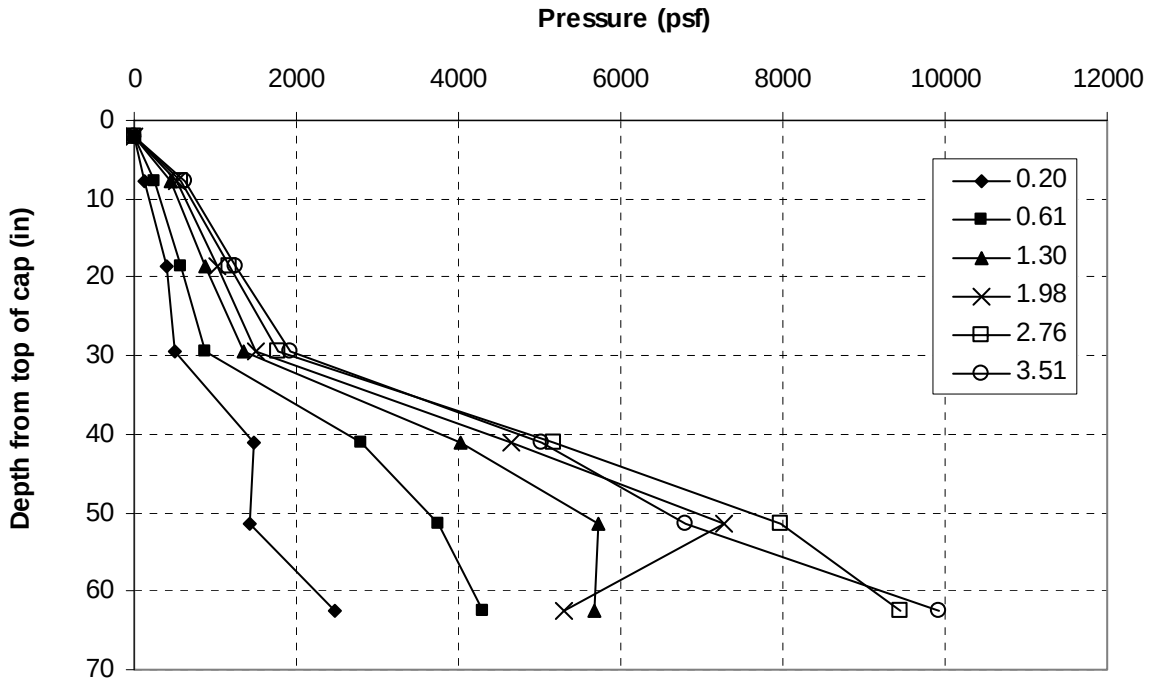

(b)

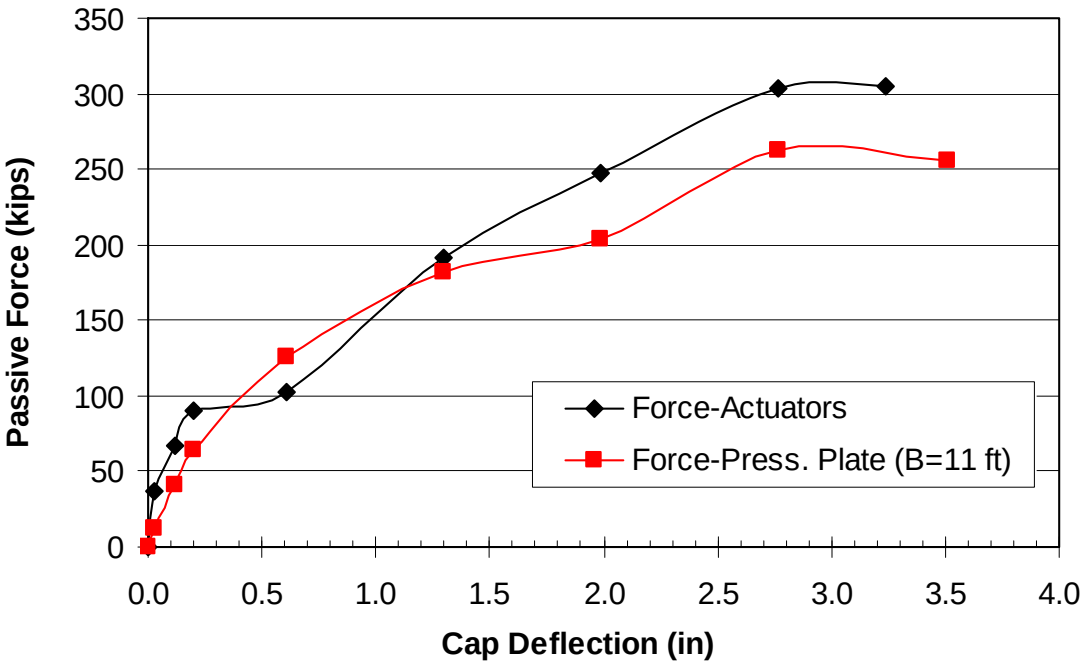

Figure 2. Pile cap test with MSE wingwalls: (a) Pressure versus depth curves for various displacement increments and (b) comparison of force-displacement curves with force obtained from the actuators and with force computed from the pressure plates times the tributary area.

(a)

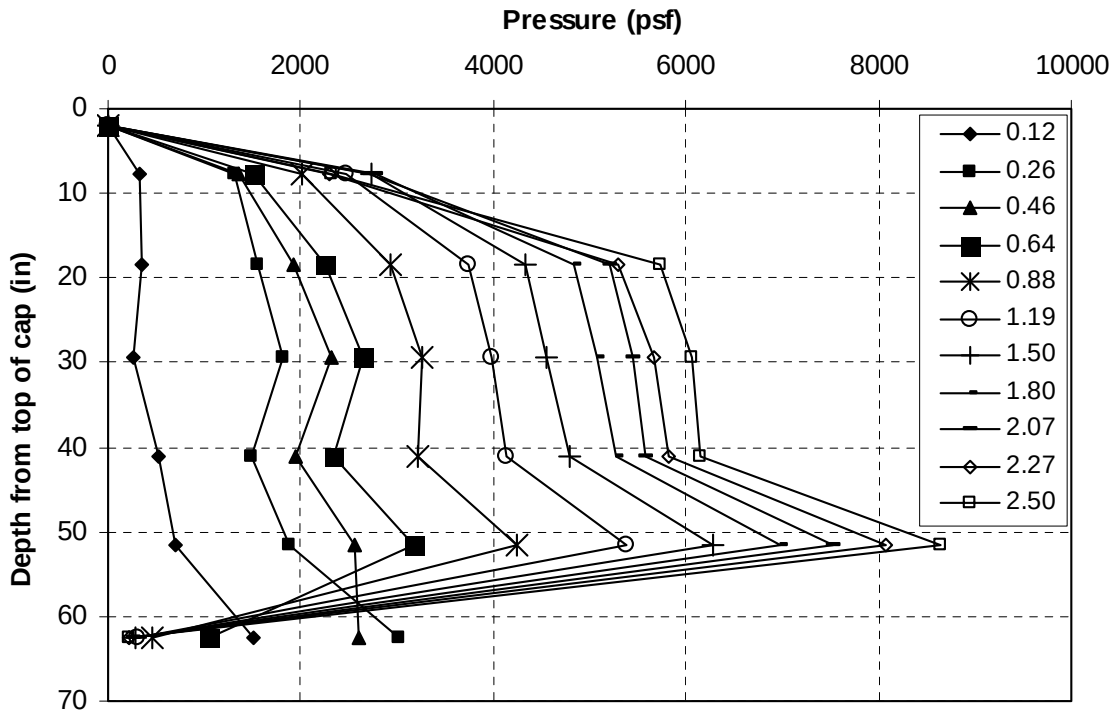

(b)

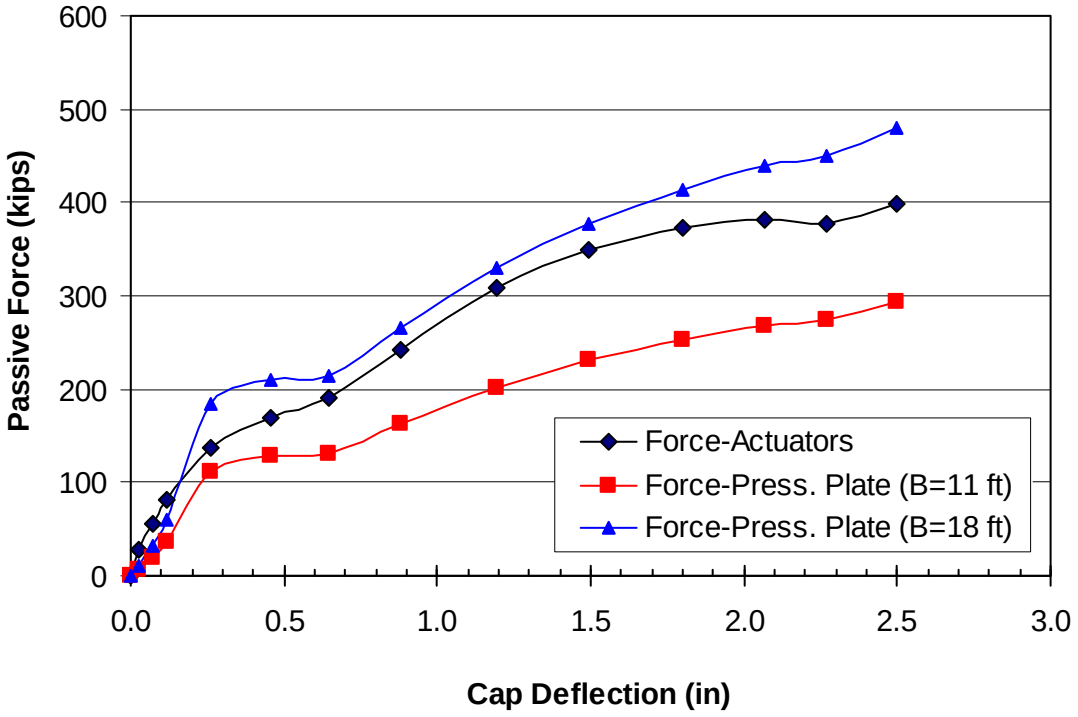

Figure 3. Pile cap test without MSE wingwalls: (a) Pressure versus depth curves for various displacement increments and (b) comparison of force-displacement curves with force obtained from the actuators and with force computed from the pressure plates times the tributary area using actual with (11 ft) and effective width (18 ft).

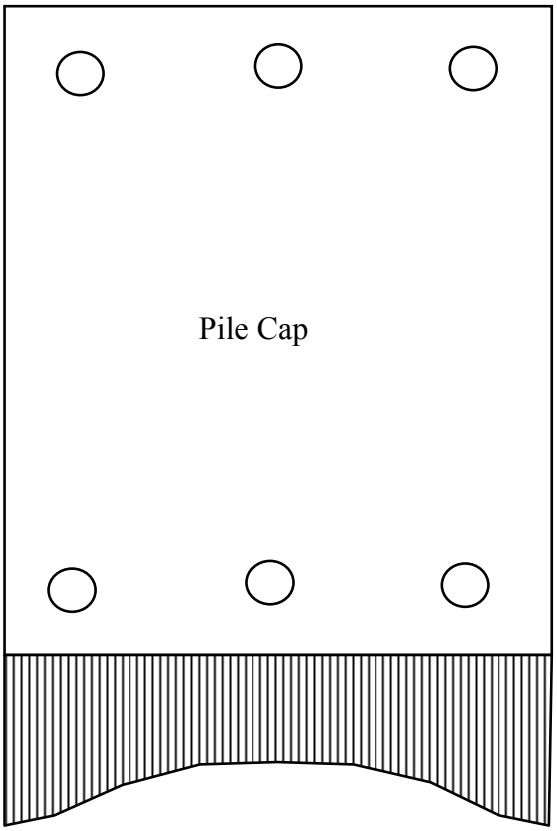

Figure 4. Schematic plan view drawing of pile cap showing stress concentrations at edges of the cap due to shear zones extending beyond the end of the cap and increasing the effective cap width.

STRAIN GAUGE INSTRUMENTATION ON MSE REINFORCEMENT AND TEST RESULTS

Strain Gauge Layout on MSE Reinforcement

The MSE wall panels were 12-ft x 5-ft x 6-in reinforced concrete. To match the height of the cap, pieces of 2x8 sawn lumber were used to extend the height of the wall panels by one-half foot. The sand backfill was compacted to 96% of the modified Proctor maximum unit weight. During the backfill construction process, two rows of galvanized steel reinforcing grids (4 grids per panel and 16 grids total) were placed at heights of 1.33 and 3.83 ft from the bottom of the MSE wall. Typical wall panel and connection details are provided in Fig. 5. The steel grids consisted of five longitudinal bars (W11-3/8 inch dia.) spaced at 8 inches on centers to form a 32 inch wide panel, 5.5 ft long. Transverse reinforcement bars (W8-5/16 inch dia.) were welded to the longitudinal bars at 12 inch spacing on centers. The edge of the first grid was approximately 12 inches from the pile cap face. The grid reinforcement was designed according to FHWA standards to have a factor of safety of 1.5 and was embedded into the backfill 5.5 ft., midway of the pile cap width.

Strain gauges were used to instrument six of the reinforcement grids so that the axial force in the reinforcement could be determined. Four of the instrumented grids were attached to the panel closest to pile cap on the east side, while the remaining two were attached to the top and bottom connections for the next panel. For each of the six steel grids, seven stain gauges were attached to one side of the center longitudinal bar at various distances from the connection to the wall panel. For the top steel grids, strain gauges were placed at distances of 2, 7, 12, 18, 30, 42, and 54 inches from the connection to the wall panel and in bottom grids, strain gauges were located at 2, 4, 6, 9, 22, 35, and 48 inches from the wall panel connection. The strain gauges were electrical resistance type gauges rather than vibrating wire gauges to allow for rapid measurement of strain during dynamic and cyclic loading.

Test Results from MSE Reinforcement Strain Gauges

The axial force in each steel reinforcing bar was computed by multiplying the measured strain at each strain gauge by the cross-section area of the bar and the elastic modulus of the steel. The total axial force for the grid was then computed by multiplying the force in the bar by the ratio of the total grid width to the tributary area for the single bar. The total force in the grid computed by this procedure is shown for the top and bottom reinforcements at three pile cap displacement increments during the pile cap test in Figure 6. In addition, the theoretical pull-out resistance as a function of distance along the length of the steel grid is shown on the plots in Figure 6 for comparison. When the pile cap had displaced only 0.6 inches into the backfill, the pullout force in both the steel grids was at or somewhat higher than the theoretical pull-out force within the essentially all of the development length. This corresponds to the point when the wall panels started moving outward and the point where there was a plateau in the passive force-displacement curve for the pile cap as shown in Figure 7.

Unfortunately, it appears that the force in the steel grid near the wall face may be influenced by bending in the reinforcing which would artificially increase the measured force.

Bending stresses can be eliminated by having strain gauges on both top and bottom faces of the grid, but this doubles the cost of the strain gauges and/or reduces the number of points where force measurements can be made. Therefore, these forces are likely higher than they really are and account for the measured forces being significantly higher than the theoretical pullout force at distances close to the wall face. The forces in the reinforcing grids increase only slightly in most cases as the pile cap displacement increases. This is likely a result of the grids pulling out and allowing the wall to move outward so that the force in the steel grids remains essentially the same.

A schematic diagram illustrating the mechanisms involved in increasing the force in the steel reinforcing grids is shown in Figure 8. As the pile cap is loaded into the backfill, passive pressure develops at the pile cap-backfill interface. The passive pressure and longitudinal displacement lead to a corresponding increase in pressure in the transverse direction. This pressure is resisted by increased force in the steel reinforcing grids which are holding the MSE wall in place. Once the pull-out force on the steel reinforcing grid is exceeded (i.e. the factor of safety against pullout is overcome), the wall simply moves laterally. As the pile cap continues to push into the backfill, the MSE wall continues to move outward, because no additional pull-out resistance is available. The authors are not aware of any method currently available in the literature which would allow a designer to predict the magnitude of increased force which might develop on a MSE wall reinforcement as a result of loading of an abutment wall transverse to the reinforcement. Obviously, the pull-out factor of safety of 1.5 in this case was insufficient to prevent grid pull-out and displacement of the MSE wall. Increasing the factor of safety against pull-out would tend to reduce displacement of the MSE wall; however, increasing the stiffness of the wall in this manner might also attract additional pressure to the wall during the loading of the pile cap. To provide designers with some means of predicting the increased pressure on the MSE wall and restricting wall movement to acceptable levels, additional field testing would be desirable with walls having progressively higher factors of safety against reinforcement pull-out.

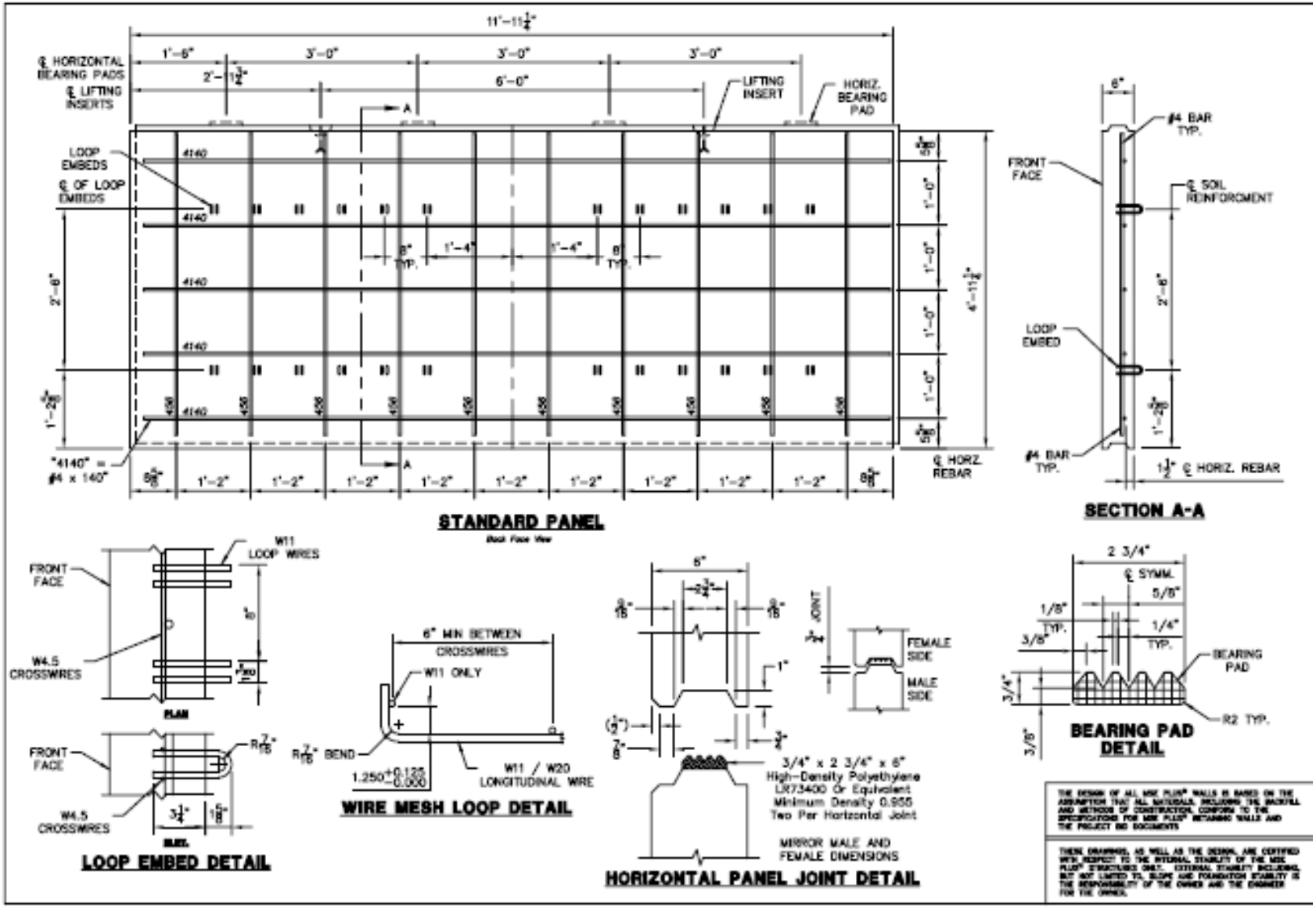

Figure 5. Plans for wall panels and connection details.

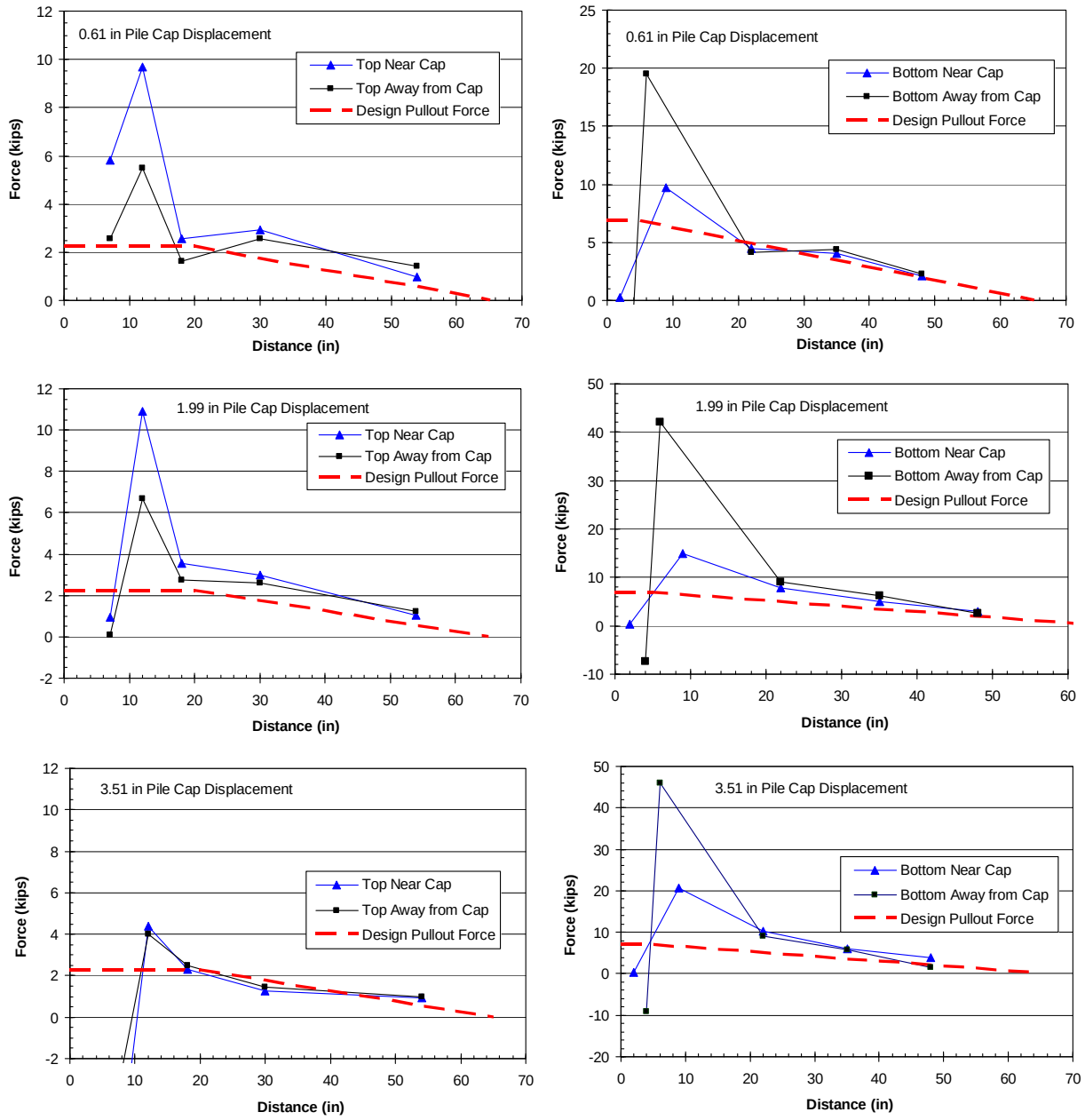

Figure 6. Summary of steel reinforcing grid force versus distance from the wall panel connection in comparison to the theoretical design pullout force for top and bottom grids at pile cap displacements of 0.61, 1.99, and 3.5 inches.

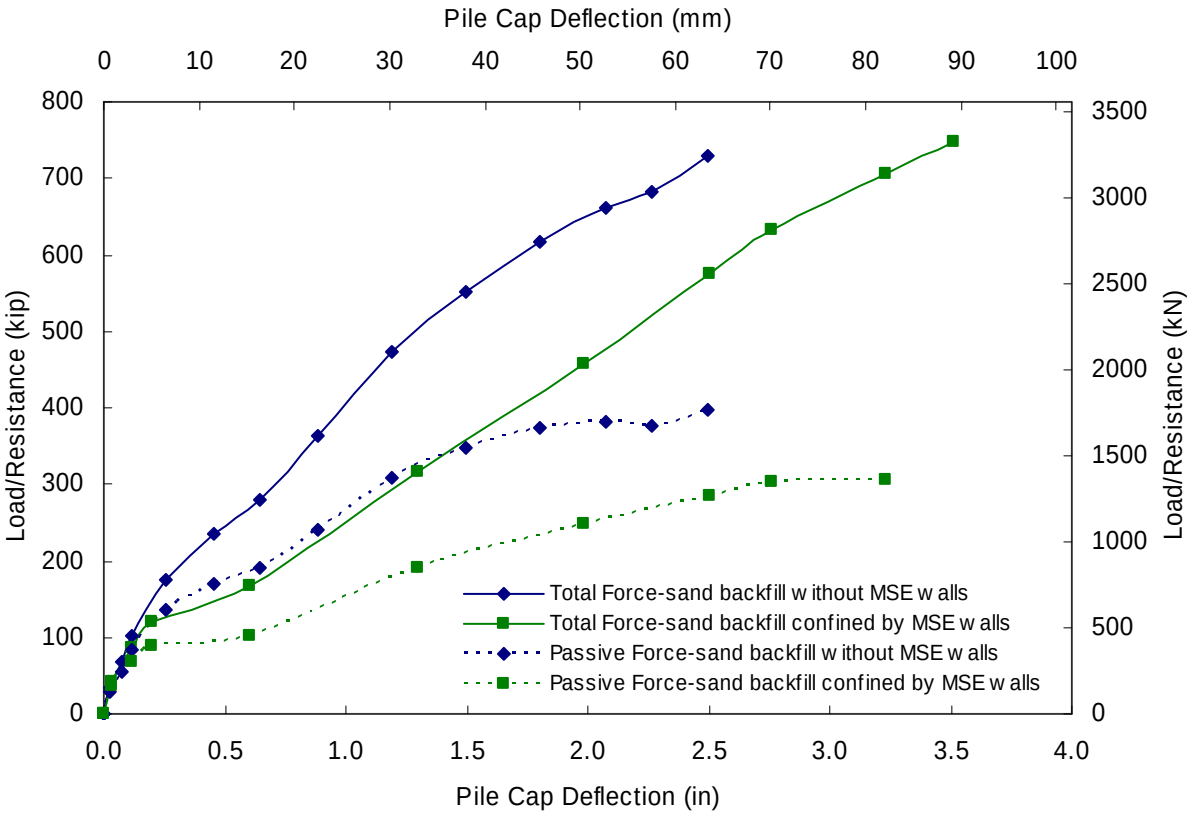

Figure 7. Total and passive force versus deflection curves.

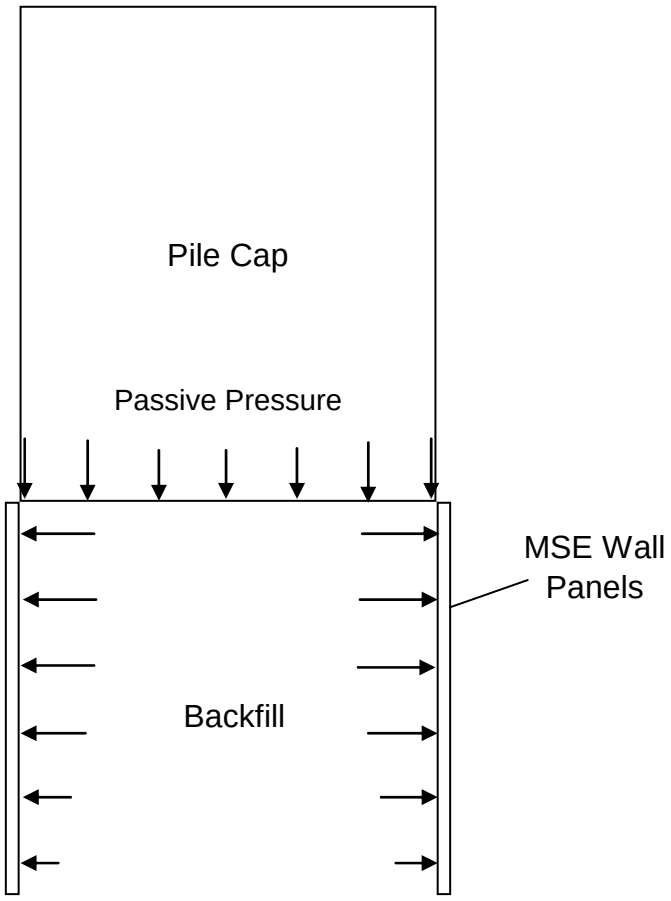

Figure 8. Schematic drawing showing how increased lateral pressure would be produced on the MSE wall as a result of longitudinal displacement and passive pressure development on the pile cap.